

RAPID COMMUNICATION

Facile synthesis of nanocrystalline hexagonal tungsten trioxide from metallic tungsten powder and hydrogen peroxide

Isao Tsuyumoto 

Department of Applied Chemistry,
College of Bioscience and Chemistry,
Kanazawa Institute of Technology,
Nonoichi, Ishikawa, Japan

Correspondence

Isao Tsuyumoto, Department of Applied
Chemistry, College of Bioscience and
Chemistry, Kanazawa Institute of
Technology, Ishikawa, Japan.
Email: tsuyu@neptune.kanazawa-it.ac.jp

Funding information

Grant-in-Aid for Scientific Research (C)
from the Japan Society for the Promotion
of Science (JSPS), Grant/Award Number:
No. 16K05946

Abstract

A hexagonal form of tungsten trioxide (h-WO₃, particle size: 15.9–57.1 nm) was found to be formed by a direct reaction between metallic tungsten powder (W, particle size: 0.45–0.59 μm) and 15%–30% hydrogen peroxide (H₂O₂) aq solution. Oxide film on the powder surface having the similar crystal structure as h-WO₃ was essential for the formation, and the surface oxide film was formed by aging the powder in air at 45°C, a relative humidity of 100% (*P*_{H₂O} 96 hPa) for 3–28 days or in ambient atmosphere at room temperature for 12 years. The Rietveld analysis performed in the space group *P6₃/mcm* (*Z* = 6) indicated the crystal structures were the same as those of the reported h-WO₃ and that the crystallographic characteristic was as follows: *a* = 0.74219 nm, *c* = 0.77198 nm for h-WO₃ from the 28-day aged powder, and *a* = 0.74538 nm, *c* = 0.77194 nm for h-WO₃ from the 12-year aged powder.

KEYWORDS

nanoparticles, oxides, synthesis, tungsten/tungsten compounds, X-ray methods

1 | INTRODUCTION

Tungsten trioxide, WO₃, has received much attention for a wide variety of applications such as photocatalyst in water splitting,^{1–8} dye-sensitized solar cells,⁹ electrode materials for lithium-ion batteries,¹⁰ photochromic films,¹¹ and electrochromic displays.^{12,13} Many methods have been reported for the preparation of WO₃ nanoparticles as well as their properties and applications.¹⁴ Tungsten trioxide crystallizes in several polymorphic forms, which can be categorized into two general crystal structures. One is based on the ReO₃-type structure, i.e., WO₆ octahedra link together by corner sharing and form a three-dimensional framework. In this case, distortions of the octahedra bring about lower symmetries than ReO₃, and these polymorphs have been reported to be monoclinic phase (II) from 5 to 278 K, triclinic phase from 248 to 290–300 K, monoclinic phase (I) (*γ*-phase) from 290–300 K to 600 K, orthorhombic phase from 600 to 1010 K, and tetragonal phase from 1010 K to the melting point, 1746 K.¹⁵ The other general crystal structure is a form with hexagonal symmetry first reported

by Gerand et al,¹⁶ i.e., WO₆ octahedra share their corners to form a framework with hexagonal channels along *c*-axis. This hexagonal WO₃ (h-WO₃) is a metastable phase, which has not been described in phase diagrams, and its synthetic routes are limited to low-temperature processes because high temperature causes transformation to the stable monoclinic phase (I).¹⁷ The h-WO₃ was first prepared by dehydration of WO₃·1/3H₂O, and this hydrate was obtained by hydrothermal treatment of an aqueous suspension of either tungstic acid gel or WO₃·2H₂O at 120°C.¹⁶ The h-WO₃ has been also prepared by other methods such as hydrogen peroxide oxidation of hexagonal ammonium tungsten bronze,¹⁸ and thermal decomposition of ammonium peroxo-polytungstate.¹⁷ These preparation processes of h-WO₃ require precise control of experimental conditions and are not suitable for inexpensive large-scale production. As the h-WO₃ as well as the monoclinic phase (I) has attracted a lot of attention as an alternative material for photocatalyst,³ a facile and inexpensive preparation method of h-WO₃ is highly desirable. Our research group has been investigating a soft-chemical synthesis of metal oxides starting from a

peroxo-metallic acid solution obtained by the direct reaction between metal powder and hydrogen peroxide.¹⁹⁻²⁶ Using such new methods we have successfully prepared K_xWO_3 ,²⁷ $BaTiO_3$,²⁸ $KNbO_3$,²⁹ $LiVO_2$,³⁰ Ramsdellite Li_xTiO_2 ,³¹ etc. In this study, we found that a direct reaction between tungsten (W) powder and 15%-30% hydrogen peroxide (H_2O_2) aq gave a precipitate of h- WO_3 instead of a peroxo-polytungstic acid solution when metallic tungsten powder with smaller particle size, 0.45-0.59 μm , was used.

2 | EXPERIMENTAL PROCEDURE

2.1 | Raw materials

Two types of metallic tungsten powders with different particle sizes were used: 0.45-0.59 μm (99.9% purity, W-H, Japan New Metals Co., Ltd., Osaka, Japan), and 1.28 μm on average (99.9% purity, No. 64401, Mitsuwa Chemicals Co., Ltd., Osaka, Japan). As for the tungsten powder with particle size of 0.45-0.59 μm , we also used an old sample stored in a sample bottle in ambient atmosphere at room temperature for 12 years along with the new samples. Hydrogen peroxide solution (30.0 wt%, Kanto Chemical Co., Inc., Tokyo, Japan) was used as purchased without further purification.

2.2 | Pretreatment

Tungsten powders were pretreated before the reaction to enhance the formation of surface oxide film having the similar crystal structure as h- WO_3 . We carried out either of the following pretreatments: heating in air at 45°C; water vapor pressure (P_{H_2O}) 96 hPa (relative humidity, RH 100%) for 1, 3, 7, 14, 21, or 28 day(s); heating in air at 275°C, P_{H_2O} 23 hPa for 12 hours; or keeping in water at 20°C for 7 days, 100°C for 12 hours, or 100°C at 1 MPa for 12 hours. The old tungsten powder stored for 12 years was used without any pretreatment.

2.3 | Synthesis

A vigorous reaction occurred by adding 11.0 g of tungsten powder into 50 mL of 15% H_2O_2 aq, and a precipitate was formed. After the vigorous reaction ceased, 20 mL of 30% H_2O_2 aq was added more to complete the reaction. The precipitate was filtrated using a membrane filter with pore size of 0.1 μm , rinsed with water, and dried at 45°C for 2 hours.

2.4 | Characterization

The X-ray diffraction (XRD) patterns of the products were measured with a diffractometer (XD-D1, Shimadzu, Kyoto,

Japan) using graphite-monochromatized CuK_α radiation ($\lambda = 0.15406$ nm). The X-ray profiles were collected between 2° and 120° of 2 θ angles with a step interval of 0.02° and a count time of 4 s/step. The crystalline parameters were refined by the Rietveld method using the RIE-TAN-FP program,^{32,33} and the crystallite sizes were estimated by the Scherrer equation. The morphology was observed by a field emission scanning electron microscope (FE-SEM, JSM-7100F, JEOL, Tokyo, Japan) with an accelerating voltage of 10 kV. The specific surface area of h- WO_3 was measured by the Brunauer-Emmett-Teller (BET) method using the adsorption of nitrogen gas at the temperature of liquid nitrogen (Micrometrics Tristar 3020, Shimadzu, Kyoto, Japan). Prior to the measurements, the samples were degassed at 200°C for 2 hours under vacuum. The thermal behavior was investigated by thermogravimetry (TG) and differential thermal analysis (DTA; DTG-50, Shimadzu, Kyoto, Japan) at a heating rate of 20°C/min in air.

3 | RESULTS AND DISCUSSION

A pale blue precipitate was found to be formed after a vigorous reaction between the old tungsten powder (particle size: 0.45-0.59 μm) stored for 12 years and hydrogen peroxide, while the reaction between the tungsten powder (particle size: 1.28 μm) and hydrogen peroxide yielded yellow transparent peroxo-polytungstic acid solution as reported in literature.^{21,22} As shown in Figure 1, the XRD pattern of the precipitate was in good agreement with that of h- WO_3 (PDF-000331387), and interestingly the old tungsten powder for the raw material showed weak broad peaks at the same angles with h- WO_3 as well as strong sharp peaks of metallic tungsten. Oxide film having the similar crystal structure as h- WO_3 was formed on the powder surface during the storage for 12 years, and this suggests that the oxide film grown on tungsten surface in ambient atmosphere at room temperature is the phase of h- WO_3 . On the other hand, the pristine tungsten powder (particle size: 0.45-0.59 μm) showed no broad peaks at the angles of h- WO_3 in the XRD pattern, and the precipitate of the same reaction became the mixture of tetragonal $WO_{2.90}$ (PDF-000181417) and other oxides. These results suggest that the oxide film on the powder surface is an essential seed crystal for the formation of h- WO_3 .

In order to prepare the surface oxide film artificially in a short time and to reproduce the formation of h- WO_3 , we aged the pristine tungsten powders (particle size: 0.45-0.59 μm) in various conditions such as steaming and boiling at ordinary and high pressures. As shown in Table 1 and Figure 2, we successfully obtained h- WO_3 as a single-phase precipitate in the reaction with hydrogen

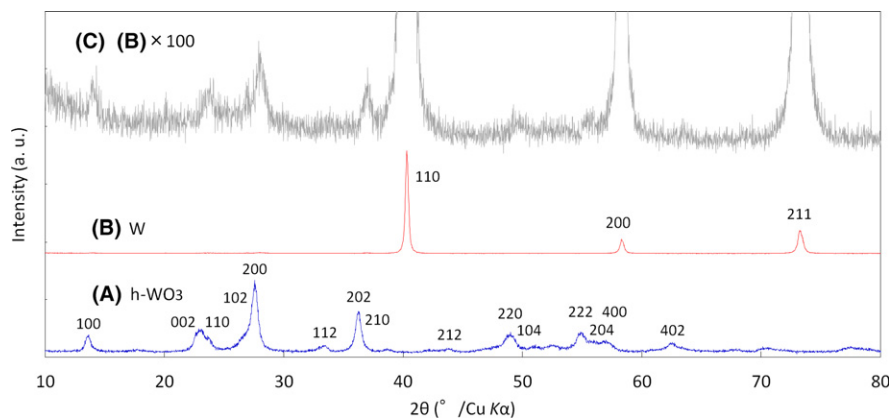


FIGURE 1 XRD patterns of (A) h-WO₃ obtained as a precipitate by the reaction between tungsten powder (particle size: 0.45–0.59 μm) stored in ambient atmosphere at room temperature for 12 years and hydrogen peroxide, (B) tungsten powder stored in ambient atmosphere at room temperature for 12 years, and (C) magnified view ($\times 100$) of (B) [Color figure can be viewed at wileyonlinelibrary.com]

peroxide by using the tungsten powder after aging at 45°C, RH 100% ($P_{\text{H}_2\text{O}}$ 9.58 kPa) for 3 days or more. Small amount of h-WO₃ (PDF-000331387) was observed along with WO₃·H₂O (PDF-000430679) and metallic tungsten (PDF-000040806) in the XRD patterns of the samples after aging at 45°C, RH 100% for 3 days or more, while the sample after aging in the same condition for 1 day showed no peaks other than those of metallic tungsten. This indicates that surface oxide film consisting of WO₃·H₂O and h-WO₃ was formed on the powder surface at 45°C in humid air and that this acted as a seed crystal for the formation of h-WO₃. After the reaction with hydrogen peroxide, WO₃·H₂O and metallic tungsten completely transformed into h-WO₃, and they were not observed in the XRD patterns of the product. When tungsten powder was aged in water at 100°C, small amount of highly crystalline WO₃·H₂O was observed together with small amount of h-WO₃ in the XRD pattern, and the highly crystalline

WO₃·H₂O on the powder surface presumably caused the predominant formation of WO₃·H₂O compared with h-WO₃. On the other hand, when the tungsten powder was aged at 275°C in humidified air for 12 hours, small amount of triclinic WO₃ (PDF-000321395) was observed on the powder surface and the triclinic WO₃ was formed after reaction with hydrogen peroxide. Furthermore, when we used tungsten powder with larger particle size, 1.28 μm, only small amount of highly crystalline WO₃·H₂O was observed together with those of W after aging at 45°C, RH 100% for 3 or 7 days, and WO₃·H₂O was obtained alone as a precipitate by the reaction with hydrogen peroxide. The precipitation of h-WO₃ occurred only when ultrafine tungsten powder with particle size of 0.45–0.59 μm was used. The surface oxide film consisting of h-WO₃ was formed only on the surface of ultrafine tungsten powder, and the film was an essential seed crystal for the formation of h-WO₃. It can be considered that the crystal growth of

TABLE 1 Aging conditions of tungsten powders (particle size: 0.45–0.59 μm) and the products after aging and reaction with hydrogen peroxide

| t (°C) | Atmosphere/solvent | $P_{\text{H}_2\text{O}}$ (hPa) | Duration | Product after aging | Main product after reaction |
|----------|--------------------|--------------------------------|----------|---|--|
| 45 | Air | 96 | 1 d | WO ₃ ·H ₂ O | WO ₃ ·H ₂ O ₂ ·H ₂ O |
| | | | 3 d | WO ₃ ·H ₂ O + h-WO ₃ | h-WO ₃ |
| | | | 7 d | WO ₃ ·H ₂ O + h-WO ₃ | h-WO ₃ |
| | | | 14 d | WO ₃ ·H ₂ O + h-WO ₃ | h-WO ₃ |
| | | | 21 d | WO ₃ ·H ₂ O + h-WO ₃ | h-WO ₃ |
| | | | 28 d | WO ₃ ·H ₂ O + h-WO ₃ | h-WO ₃ |
| 275 | Air | 23 | 12 h | Triclinic WO ₃ | Triclinic WO ₃ |
| 20 | Water | — | 7 d | WO ₃ ·H ₂ O | WO ₃ ·H ₂ O |
| 100 | Water | — | 12 h | WO ₃ ·H ₂ O + h-WO ₃ | WO ₃ ·H ₂ O + h-WO ₃ |
| 100 | Water, 1 MPa | — | 12 h | WO ₃ ·H ₂ O | WO ₃ ·H ₂ O |

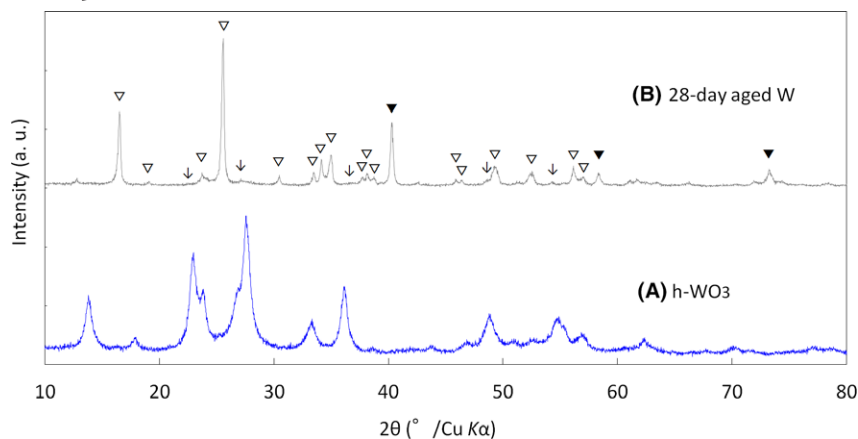


FIGURE 2 XRD patterns of (A) h-WO₃ obtained as a precipitate by the reaction between tungsten powder (particle size: 0.45–0.59 μm) aged in air at 45°C and a relative humidity of 100% ($P_{\text{H}_2\text{O}}$ 9.58 kPa) for 28 days and hydrogen peroxide, and (B) tungsten powder (particle size: 0.45–0.59 μm) aged in air at 45°C and a relative humidity of 100% ($P_{\text{H}_2\text{O}}$ 9.58 kPa) for 28 days. ▼: W, ▽: WO₃·H₂O, ↓: h-WO₃ [Color figure can be viewed at wileyonlinelibrary.com]

the metastable phase, h-WO₃, is easy to occur on the low crystalline metal surface of ultrafine powder rather than the high crystalline surface of the larger particles. The Rietveld refined structural parameters for h-WO₃ from two types of tungsten powders after storage for 12 years and after aging for 28 days at 45°C, RH 100% are summarized in Table 2. All the data were well fitted with the space group $P6_3/mcm$ ($Z = 6$), and the crystal structures proved to be similar to those in the earlier reports.^{11,12} Gerand et al described the structure using the space group $P6/mmm$ ($Z = 3$), and the O(1) atoms between the W layers were fixed at 3 g sites ($1/2, 0$, and $1/2$) with high symmetries. We located the O

(1) atoms at 6 g sites ($x, 0, 1/4$) with lower symmetries in the space group $P6_3/mcm$ ($Z = 6$) and obtained the structural parameter, $x: 0.500(7)$, as fitting results for the both samples. The O(1) atoms positions converged to the same atomic positions as the 3 g sites ($1/2, 0$, and $1/2$) in the

TABLE 2 Refined crystallographic data of h-WO₃ obtained from tungsten powder aged for 12 years (A) and aged at 45°C, RH 100% for 28 days (B)

| (a) Hexagonal; space group; $P6_3/mcm$ (193) | | | |
|--|-----------------------|-----------------|--|
| $a = 0.74538(16)$ nm, $c = 0.77194(20)$ nm $Z = 6$ | | | |
| Atom | Site | Atomic position | Occupancy |
| W | 6 f ($1/2, 0, 0$) | | 1.0 |
| O(1) | 6 g ($x, 0, 1/4$) | $x: 0.500(7)$ | 1.0 |
| O(2) | 12 i ($x, 2x, 0$) | $x: 0.1982(16)$ | 1.0 |
| Interatomic distances/nm | | | |
| W-O(1) | 2×0.1930 | O(1)-O(2) | 8×0.2765 |
| W-O(2) | 4×0.1980 | O(2)-O(2) | 2×0.2559 2×0.3021 |
| (b) Hexagonal; space group; $P6_3/mcm$ (193) | | | |
| $a = 0.74219(13)$ nm, $c = 0.77198(13)$ nm $Z = 6$ | | | |
| Atom | Site | Atomic position | Occupancy |
| W | 6 f ($1/2, 0, 0$) | | 1.0 |
| O(1) | 6 g ($x, 0, 1/4$) | $x: 0.500(3)$ | 1.0 |
| O(2) | 12 i ($x, 2x, 0$) | $x: 0.1913(15)$ | 1.0 |
| Interatomic distances/nm | | | |
| W-O(1) | 2×0.1930 | O(1)-O(2) | 8×0.2783 |
| W-O(2) | 4×0.2003 | O(2)-O(2) | 2×0.2459 2×0.3163 |

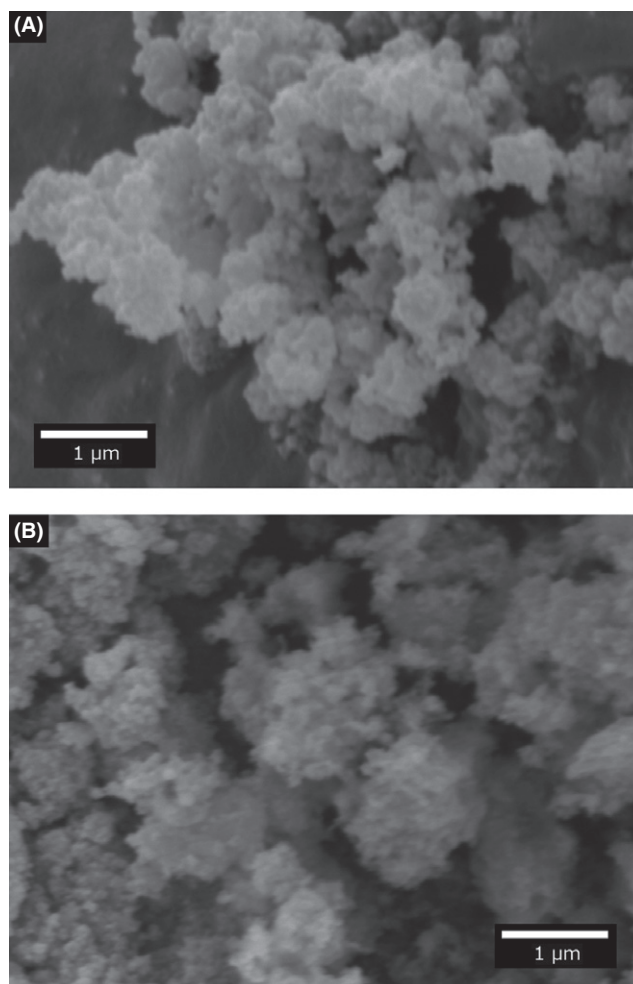


FIGURE 3 FE-SEM images of h-WO₃ powders prepared from tungsten powders stored for 12 years (A) and aged at 45°C, and RH 100% for 28 days (B)

space group $P6/mmm$, and consequently we obtained the same fitting results for the two space groups $P6_3/mcm$ and $P6/mmm$. The result for the space group $P6_3/mcm$ is presented here because this is more supportive of the atomic position of O(1). The interatomic distances between W and O were calculated at 0.1980–0.2003 nm along the ab plane and 0.1930 nm along the c -axis, and these are in good agreement with the reported W–O single bonding distances.^{12,22} The O–O distances between neighboring oxygens vary from 0.2459 nm to 0.3163 nm, and this brings about the distortion of the WO_6 octahedra, which are stacked parallelly to the c -axis. Additionally, Oi et al used more general sites of the same space group $P6_3/mcm$ and reported remarkably distorted WO_6 octahedra. We also considered such atomic arrangement, but the fitting results were either almost the same as the above results or divergent. Thus, we adopted the present atomic arrangement. The crystallite sizes of h- WO_3 estimated from the peak profile parameters using the Scherrer equation were 14.2 nm and 12.6 nm, respectively, for the samples from 12-year-old tungsten powder and from 28-day aged tungsten powder. The BET specific surface areas of h- WO_3 were 16.9 m²/g and 60.3 m²/g, respectively, for the samples from 12-year-old tungsten powder and from 28-day aged tungsten powder. If we assume spherical particles, the average particle sizes are calculated at 57.1 nm and 15.9 nm, respectively. Figure 3 shows the FE-SEM images of h- WO_3 powders prepared from 12-year-old tungsten powder and from 28-day aged tungsten powder. The aggregates of nanocrystalline particles are observed for both of the samples. The crystallite size of h- WO_3 from 28-day aged tungsten powder was smaller than that from 12-year-old tungsten powder, and this is in good agreement with the results obtained from the BET analysis. The crystallite sizes of both of h- WO_3 were much smaller than the particle size of the raw material tungsten powder (0.45–0.59 μ m) and varied depending on the preparation method. This suggests that the formation process of h- WO_3 is a topochemical oxidation through powder surface involving disruption to nanocrystalline particles. This room-temperature process allowed the formation of nanocrystalline and metastable phase by suppressing further crystal growth and transformation into more stable phase. This method is advantageous in preparation of nanocrystalline and metastable metal oxides because a high-temperature crystal growth process is not involved in the reaction unlike the solid-state reactions and the hydrothermal methods.

4 | CONCLUSIONS

Nanocrystalline h- WO_3 with crystallite size of 12.6–14.2 nm was facilely obtained as a precipitate in the direct reaction

between tungsten powder and hydrogen peroxide. This new synthetic route necessitates surface oxide film having the similar crystal structure as h- WO_3 , which can be obtained by aging the tungsten powder under conditions such as in air at 45°C, RH 100% for 3–28 days. The surface oxide film acts as a seed crystal for the crystal growth and leads to the formation of the metastable phase. The crystal structure of the present h- WO_3 was well fitted with the space groups $P6_3/mcm$ and $P6/mmm$ in the Rietveld refinement and confirmed to be the same as that first reported by Gerand et al. Our method is advantageous over the conventional ones in that it is a facile room-temperature process and allows the formation of metastable and nanocrystalline phases. We consider the method will be applied to the preparation of the other metal oxides by using direct reactions of metallic powders such as titanium, molybdenum, niobium, and vanadium with hydrogen peroxide.

ACKNOWLEDGMENTS

The author is sincerely grateful to Mr. A. Edano and Mr. T. Kousaka for experimental assistance and to Prof. M. Sakamoto for the FE-SEM measurement. This work was supported by a Grant-in-Aid for Scientific Research (C), No. 16K05946, from the Japan Society for the Promotion of Science (JSPS).

ORCID

Isao Tsuyumoto  <http://orcid.org/0000-0003-1644-6077>

REFERENCES

1. Li Y, Wang C, Zheng H, et al. Surface oxygen vacancies on WO_3 contributed to enhanced photothermo-synergistic effect. *Appl Surf Sci.* 2017;391:654–661.
2. Kumar SG, Rao KSRK. Comparison of modification strategies towards enhanced charge carrier separation and photocatalytic degradation activity of metal oxide semiconductors (TiO_2 , WO_3 and ZnO). *Appl Surf Sci.* 2017;391:124–148.
3. Lee T, Lee Y, Jang W, Soon A. Understanding the advantage of hexagonal WO_3 as an efficient photoanode for solar water splitting: a first-principles perspective. *J Mater Chem A.* 2016;4:11498–11506.
4. Jin J, Yu J, Guo D, Cui C, Ho W. A hierarchical Z-scheme $CdS-WO_3$ photocatalyst with enhanced CO_2 reduction activity. *Small.* 2015;11:5262–5271.
5. Coridan RH, Shaner M, Wiggenshorn C, Brunschwig BS, Lewis NS. Electrical and photoelectrochemical properties of WO_3/Si tandem photoelectrodes. *J Phys Chem C.* 2013;117:6949–6957.
6. Waller MR, Townsend TK, Zhao J, et al. Single-crystal tungsten oxide nanosheets: photochemical water oxidation in the quantum confinement regime. *Chem Mater.* 2012;24:698–704.
7. Walter MG, Warren EL, McKone JR, et al. Solar water splitting cells. *Chem Rev.* 2010;110:6446–6473.

8. Maeda K, Higashi M, Lu D, Abe R, Domen K. Efficient nonsacrificial water splitting through two-step photoexcitation by visible light using a modified oxynitride as a hydrogen evolution photocatalyst. *J Am Chem Soc.* 2010;132:5858-5868.
9. Zheng H, Tachibana Y, Kalantar-zadeh K. Dye-sensitized solar cells based on WO_3 . *Langmuir.* 2010;26:19148-19152.
10. Yin J, Cao H, Zhang J, Qu M, Zhou Z. Synthesis and applications of γ -tungsten oxide hierarchical nanostructures. *Cryst Growth Des.* 2013;13:759-769.
11. Gavriluyk AI. Aging of the nanosized photochromic WO_3 films and the role of adsorbed water in the photochromism. *Appl Surf Sci.* 2016;364:498-504.
12. Li H, Wang J, Shi Q, et al. Constructing three-dimensional quasi-vertical nanosheet architectures from self-assemble two-dimensional $\text{WO}_3 \cdot 2\text{H}_2\text{O}$ for efficient electrochromic devices. *Appl Surf Sci.* 2016;380:281-288.
13. Chang X, Sun S, Dong L, Hu X, Yin Y. Tungsten oxide nanowires grown on graphene oxide sheets as high-performance electrochromic material. *Electrochim Acta.* 2014;129:40-46.
14. Ahmadi M, Younesi R, Guinel M. Synthesis of tungsten oxide nanoparticles using a hydrothermal method at ambient pressure. *J Mater Res.* 2014;29:1424-1430.
15. Cazzanelli E, Vinegoni C, Mariotto G, Kuzmin A, Purans J. Low-temperature polymorphism in tungsten trioxide powders and its dependence on mechanical treatments. *J Solid State Chem.* 1999;143:24-32.
16. Gerand B, Nowogrocki G, Guenet J, Figlarz M. Structural study of a new hexagonal form of tungsten trioxide. *J Solid State Chem.* 1979;29:429-434.
17. Oi J, Kishimoto A, Kudo T, Hiratani M. Hexagonal tungsten trioxide obtained from peroxo-polytungstate and reversible lithium electro-intercalation into its framework. *J Solid State Chem.* 1992;96:13-19.
18. Cheng KH, Whittingham MS. Lithium incorporation in tungsten oxides. *Solid State Ionics.* 1980;1:151-161.
19. Tsuyumoto I, Nawa K. Thermochromism of vanadium-titanium oxide prepared from peroxovanadate and peroxotitanate. *J Mater Sci.* 2008;43:985-988.
20. Tsuyumoto I, Nawa K. Thermochromism of titanium-vanadium oxide thin films prepared from peroxotitanate and peroxovanadate solutions. *Solid State Ionics.* 2008;179:1227-1229.
21. Tsuyumoto I, Kudo T. Humidity sensor using potassium hexagonal tungsten bronze synthesized from peroxo-polytungstic acid and its resistivity change mechanism. *Mater Res Bull.* 1996;31:17-28.
22. Tsuyumoto I, Kudo T. Humidity sensor using potassium hexagonal tungsten bronze synthesized from peroxo-polytungstic acid. *Sens Actuators, B.* 1996;30:95-99.
23. Kudo T, Sasaki Y, Hashimoto M, Matsumoto K. Oxalato complexes directly formed by the reaction of interstitial with hydrogen peroxide. *Inorg Chim Acta.* 1988;145:205-209.
24. Kudo T, Ishikawa A, Okamoto H, et al. Spin-coatable inorganic resists based on novel peroxopolyniobotungstic acids for bilayer lithography. *J Electrochem Soc.* 1987;134:2607-2613.
25. Kudo T, Okamoto H, Matsumoto K, Sasaki Y. Peroxopolytungstic acids synthesized by direct reaction of tungsten or tungsten carbide with hydrogen peroxide. *Inorg Chim Acta.* 1986;111:L27-L28.
26. Kudo T. A new heteropolyacid with carbon as a heteroatom in a Keggin-like structure. *Nature.* 1984;312:537-538.
27. Tsuyumoto I, Kishimoto A, Kudo T. Hexagonal tungsten bronze synthesized from potassium peroxo-polytungstate and its electrical properties. *Solid State Ionics.* 1993;59:211-216.
28. Tsuyumoto I, Kobayashi M, Are T, Yamazaki N. Nano-sized tetragonal BaTiO_3 powders synthesized by a new peroxo-precursor decomposition method. *Chem Mater.* 2010;22:3015-3020.
29. Tsuyumoto I, Arai Y, Kato T. Preparation of nanocrystalline perovskite KNbO_3 by peroxo-precursor decomposition method. *Mater Res Bull.* 2010;45:1899-1902.
30. Tsuyumoto I, Nakakura Y, Yamaki S. Nano-sized layered LiVO_2 prepared from peroxo-polyvanadic acid and its electrochemical properties. *J Am Ceram Soc.* 2014;97:3374-3377.
31. Tsuyumoto I, Moriguchi T. Synthesis and lithium insertion properties of ramsdellite Li_xTiO_2 anode materials. *Mater Res Bull.* 2015;70:748-752.
32. Momma K, Izumi F. VESTA 3 for three-dimensional visualization of crystal, volumetric and morphology data. *J Appl Crystallogr.* 2011;44:1272-1276.
33. Izumi F, Momma K. Three-dimensional visualization in powder diffraction. *Solid State Phenom.* 2007;130:15-20.

How to cite this article: Tsuyumoto I. Facile synthesis of nanocrystalline hexagonal tungsten trioxide from metallic tungsten powder and hydrogen peroxide. *J Am Ceram Soc.* 2018;101:509–514. <https://doi.org/10.1111/jace.15250>